



# A Paper-Based Multiplexed Transaminase Test for Low-Cost, Point-of-Care Liver Function Testing

## Citation

Pollock, Nira R., Jason P. Rolland, Shailendra Kumar, Patrick D. Beattie, Sidhartha Jain, Farzad Noubary, Vicki L. Wong, Rebecca A. Pohlmann, Una S. Ryan, and George M. Whitesides. 2012. A Paper-Based Multiplexed Transaminase Test for Low-Cost, Point-of-Care Liver Function Testing. *Science Translational Medicine* 4, no. 152: 152ra129.

## Published Version

doi:10.1126/scitranslmed.3003981

## Permanent link

<http://nrs.harvard.edu/urn-3:HUL.InstRepos:11933747>

## Terms of Use

This article was downloaded from Harvard University's DASH repository, and is made available under the terms and conditions applicable to Open Access Policy Articles, as set forth at <http://nrs.harvard.edu/urn-3:HUL.InstRepos:dash.current.terms-of-use#OAP>

## Share Your Story

The Harvard community has made this article openly available. Please share how this access benefits you. [Submit a story](#).

[Accessibility](#)

## **A paper-based multiplexed transaminase test: towards low-cost point-of-care liver function testing**

**Authors:** Nira R. Pollock\*†<sup>1a</sup>, Jason P. Rolland\*†<sup>2</sup>, Shailendra Kumar<sup>2</sup>, Patrick D. Beattie<sup>2</sup>, Sidhartha Jain<sup>2</sup>, Farzad Noubary<sup>3</sup>, Vicki L. Wong<sup>2</sup>, Rebecca A. Pohlmann<sup>1b</sup>, Una S. Ryan<sup>2</sup>, George M. Whitesides<sup>4</sup>

### **Affiliations:**

<sup>1a</sup>Division of Infectious Diseases and <sup>1b</sup>Division of Pathology, Beth Israel Deaconess Medical Center, 330 Brookline Avenue, Boston, Massachusetts, USA, 02215.

<sup>2</sup>Diagnostics For All, 840 Memorial Dr., Cambridge, Massachusetts, USA, 02139.

<sup>3</sup>Department of General Medicine/Division of Infectious Diseases, Massachusetts General Hospital, 55 Fruit St., Boston, Massachusetts, USA, 02114 .

<sup>4</sup>Department of Chemistry and Chemical Biology, Harvard University, 12 Oxford St., Cambridge, Massachusetts, USA, 02138.

\*To whom correspondence should be addressed: Jason P. Rolland ([jrolland@dfa.org](mailto:jrolland@dfa.org)) and Nira R. Pollock ([npollock@bidmc.harvard.edu](mailto:npollock@bidmc.harvard.edu)).

† These authors contributed equally to this work

**One Sentence Summary:** This manuscript describes a paper-based, multiplexed microfluidic assay for rapid, semi-quantitative, visual measurement of AST and ALT in clinical whole blood and serum specimens.

**Abstract:** In developed nations, monitoring for drug-induced liver injury (DILI) via serial measurements of serum transaminases (aspartate aminotransferase (AST) and alanine aminotransferase (ALT)) in at-risk individuals is standard-of-care. Despite the need, monitoring for DILI in resource-limited settings is often limited by expense and logistics, even for patients at highest risk. This manuscript describes a paper-based multiplexed microfluidic assay for rapid, semi-quantitative, visual measurement of AST and ALT in a fingerstick specimen. Using clinical specimens obtained by venipuncture, we have shown that our assay can, in 15 min, provide measurements of AST and ALT in whole blood or serum that allow the user to place those values into one of three readout “bins” (<3x upper limit of normal (ULN), 3–5x ULN, and >5x ULN, corresponding to TB/HIV treatment guidelines) with >90% accuracy. These data suggest that the ultimate point-of-care fingerstick device will have high impact on patient care.

## Introduction

Blood tests for monitoring the status of the liver are a standard part of medical care in developed nations, particularly for individuals who either have underlying liver disease or who are taking medications that can cause hepatotoxicity. Accordingly, US guidelines call for baseline and serial monitoring of serum transaminases, AST and ALT, in at-risk individuals while on standard therapies for tuberculosis (TB) (1) and/or human immunodeficiency virus (HIV) (2). The overall incidence of clinically relevant hepatotoxicity on TB therapy (typically due to the medications isoniazid, rifampin, and/or pyrazinamide) ranges from 2–33%, and risk may be increased by multiple factors, such as abnormal baseline transaminases, increasing age, pre-existent liver disease (e.g. hepatitis B and/or C), alcohol use, pregnancy, and malnutrition (1, 3). Hepatotoxicity associated with nevirapine-based antiretroviral therapy, widely used in the developing world, is of particular concern; rates of nevirapine-associated hepatotoxicity can exceed 13%, depending on underlying risk factors and treatment (2, 4, 5). Simultaneous treatment for both TB and HIV further complicates matters, and sometimes generates additive risk of hepatotoxicity (6, 7). In practice, however, it is difficult to predict accurately which patients on treatment will actually develop hepatotoxicity. For example, severe idiosyncratic drug-induced liver injury has been observed (8) in patients with no obvious predictors for isoniazid-associated liver injury who were treated with isoniazid alone for latent TB.

Monitoring for hepatotoxicity in resource-limited settings is often limited by relative expense and logistical and practical concerns, even for patients at highest risk of hepatotoxicity. Testing is often done in centralized or regional laboratories in these settings, and obtaining and acting on results can be substantially delayed. Many patients have strong negative feelings about venipuncture itself, and this aversion can be a barrier to care (9). Because of these obstacles, in

many resource-limited settings patients with TB and/or HIV receive minimal or no monitoring during treatment. A low-cost, less invasive, point-of-care (POC) transaminase test would have a dramatic impact on patient care in the developing world.

In order to maintain the advantages of low-cost and user-friendly operation necessary for universal access to POC screening, without sacrificing the ability to perform clinically useful (and even complex) tests, we (10–15), and others (16–23), have developed microfluidic platforms based on paper (broadly defined as thin, porous media). Paper-based microfluidic devices consist of hydrophilic paper channels defined by patterning of hydrophobic barriers (10, 12, 13) or by cutting (16–20, 23). Using these defined channels, fluid flow can be directed towards specific detection zones and operations such as mixing, splitting, and filtration can be performed autonomously.

The advantages of patterned paper devices over traditional POC devices include: i) the capacity for high levels of multiplexing, ii) ease of exchanging assays in individual test zones, iii) the broad availability of relevant, well-characterized materials and technology at low cost, iv) the fact that no power is required, v) the fact that paper is easily chemically modified, vi) the availability of techniques to modify and direct flow within microfluidic channels, and in three dimensions, without external pumps or instrumentation, and vii) easy portability and disposability. Paper microfluidic technology has been reported in several publications focusing on the patterning technology (10, 12, 13, 18, 21, 23), fluid behavior (16–19), and potential clinical diagnostic applications (11–24). These proof-of-principle studies have demonstrated both the ability to conduct clinical chemistry, enzymatic, immunoassay, and ELISA tests on patterned paper, visually and quantitatively (latter through the use of camera-enabled cellphones) and the viability of both single layer (12, 14, 16–24) and three-dimensional (13) patterned paper devices.

Analytes detected on patterned-paper platforms thus far have included glucose (colorimetric (10-13, 22) and electrochemical (15)), protein (bovine serum albumin) (12, 23, 24), HIV gp41 antibody (14), ketones (23), nitrites (23), AST (24), and alkaline phosphatase (24).

Despite this substantial body of proof-of-concept work, there are no data, to our knowledge, evaluating actual clinical specimens using a paper-based microfluidic device, and a field-ready clinical test has never been demonstrated.

Herein, we demonstrate major progress towards the development of a paper-based, POC assay for rapid semi-quantitative measurement of AST and ALT in a fingerstick whole blood specimen. Ours will be the first actual clinical assay developed using patterned paper technology. For highest clinical utility, the device has been optimized for visual color readout in AST and ALT ranges (“bins”) that correspond to the cutoffs (<3x ULN, 3–5x ULN, and >5x ULN) currently used for clinical management decisions per US TB (1) and HIV treatment guidelines (2). Our data suggest that ultimately, the fingerstick device will have the potential for high impact on patient care, particularly in resource-limited settings.

## **Results**

### *Design and chemistry of the paper-based transaminase test*

The paper-based transaminase test is an example of a three-dimensional device made from layering patterned paper. To create a layer of patterned paper, we used a wax-based printer and a heat source to print hydrophobic barriers into a sheet of paper in order to create microfluidic, hydrophilic paths within the paper, through which flow (drawn by wicking) can be directed to specific “detection zones.” Layers of patterned paper were stacked to generate 3-D

devices by depositing patterned layers of hydrophobic adhesive via screen printing and adhering multiple sheets together. Our postage stamp-sized device (20 x 20 x 0.5 mm) is designed to perform two separate tests from a single drop of blood; specifically, one zone measures AST and another measures ALT. Additionally, the test contains three control zones to ensure proper device performance. Each test zone has a unique environment (pH, buffer, reagents, etc). The AST assay chemistry (Supplementary Methods) is based on the sulfonation of methyl green, which results in a visual transformation from blue to pink as the dye becomes colorless and the pink background color (Rhodamine B) is revealed. The ALT assay chemistry (Supplementary Methods) is based on the conversion of l-alanine to pyruvate, the subsequent oxidation of pyruvate by pyruvate oxidase, and the utilization by horseradish peroxidase of the liberated hydrogen peroxide to generate a red dye through the coupling of 4-amino antipyrine and N,N-dimethylaminobenzoic acid.

Our device consists of two layers of similarly patterned paper, a plasma separation membrane, and a laminated cover of polyester film to protect the device from the environment and limit evaporation (Fig. 1A). A hole in the lamination allows for a fingerstick or pipetted drop (30  $\mu$ L) of whole blood (or serum) to be applied to the plasma separation membrane (Fig. 1B); if whole blood is applied, blood cells are captured and retained by the plasma separation membrane while plasma wicks into the individual “zones” in the first layer of paper below. In those zones, the plasma fluid reconstitutes dried reagents (as required for the zone-specific chemistry) and continues to wick to the second layer of paper, where analytes in the plasma react with additional dried reagents in each detection zone (Fig. S1) and generate visual colorimetric signals that can be interpreted using a visual “read guide” (Fig. 1C).

The assay is read 15 min after “activation” (application of the blood or serum specimen) by viewing the test and control zones (Fig. 1B, Fig. 2). For the ALT and AST test zones, the color present in the zone is matched to the gradient of color in the visual “read guide” to obtain a result (Fig. 1C). The read guide was generated using device images obtained from a desktop scanner and image analysis software (Methods). The paper-based transaminase test has a number of features that provide critical information to the user (Fig. 2). The test has been carefully engineered for visual read-out, in that the AST/ALT test zones provide a strong color change across the target clinical range (Fig. 1C, Fig. 2A, B). We specifically optimized the interpretable ranges for AST and ALT values (i.e. corresponding color readouts in the test zones) to correspond to the cutoffs currently used for clinical management decisions per US TB treatment guidelines (1). Accordingly, the results of the test are interpreted as being within one of the following three “bins”: <3x the upper limit of normal (ULN) (0–119 U/L), 3–5x ULN (120–200 U/L), or >5x ULN (>200 U/L)(Fig. 1C). The additional color gradation within each bin on the reading guide (Fig. 1C) allows the reader to assess approximately where within the bin the result lies, and thus allows semi-quantitative readout. Additionally, three control zones notify the user of insufficient sample volume, hemolysis, or damaged reagents (Fig. 2C–E); each zone is interpreted as “valid” or “invalid.” A result of “invalid” in any of the three control zones invalidates the entire device.

#### *Analytical performance of the prototype device in buffer, whole blood, and serum*

Linearity of the test was measured by adding known amounts of purified ALT and AST to fresh whole blood (Methods), pipetting 30  $\mu$ L of blood onto the device and digitizing the color reactions observed after 15 min using a desktop scanner. Image analysis software (ImageJ, NIH) was used to translate the resulting color intensities in each scanned zone into quantitative



information. Both assays were linear across the target clinical range (40 to 200 U/L), and the 95% prediction intervals showed that, given a particular ALT or AST value, the range of possible color intensities was relatively narrow (Fig. 3). R-squared values of 0.95 and 0.98 were measured for the ALT and AST plots, respectively (each datum represents an average of three devices).

Limit of detection (LOD) curves were generated for the AST and ALT assays (Methods) and fit to the Hill equation by non-linear regression (14). Color intensity was measured as previously described (desktop scanner/ImageJ). Intensity was measured for ALT/AST concentrations prepared in buffer spanning several orders of magnitude (N=7 measurements per point). The calculated LOD was 53 U/L for the ALT assay and 84 U/L for the AST assay (Fig. 4).

To measure repeatability of the paper-based test, color intensity was measured (scanner/ImageJ) for simulated clinical samples (commercial serum samples with known AST/ALT values, and fresh whole blood samples spiked with AST/ALT (Methods) containing low/normal (“Low”) and elevated (“High”) levels of AST and ALT (Table 1). Ten devices were used to measure each sample. Precision was quantified using the coefficient of variation (%CV), defined as the standard deviation divided by the mean, for each sample. Values of the CV were < 10% for both AST and ALT tests in all four conditions (elevated/normal serum/blood)(Table 1).

#### *Performance of the prototype device in clinical specimens*

In order to measure the accuracy of the paper-based transaminase test with respect to the ability of a reader to place values measured by eye in the correct bin (<3x ULN, 3–5x ULN, or >5x ULN), a set of clinical specimens was tested. For these experiments, we tested aliquots (30

$\mu\text{L}$ ) of paired whole blood and serum specimens that had been drawn (in standard EDTA-containing and serum-separator tubes, respectively) simultaneously from Beth Israel Deaconess Medical Center (BIDMC) patients within the previous 5 h for routine clinical testing, and for which results of automated transaminase testing (Methods) of the serum specimen were available (BIDMC does not perform transaminase testing on whole blood specimens). Aliquots (30  $\mu\text{L}$ ) of blood or serum were applied to each device, and the devices were allowed to sit at room temperature (range: 21–24 °C) for 15 min. Each paper assay was then read visually by three independent readers who were blinded to automated results. The readers independently matched test zone colors to the closest color/value found on the read guide (Fig. 1C) and recorded a result in U/L (rounded to the nearest 10 U/L ; i.e. 100 U/L or 110 U/L ). (Of note, some color resolution is lost when scanning the devices. The loss in resolution results in conservatively calculated LOD values (above). Attempts to distinguish values below the calculated LODs visually were allowed, as discernible color changes, observed by eye, made it possible (in principle) to discriminate lower values (Fig. 1C). Importantly, discrimination at these lower values does not affect the resulting “bin” placement).

Results of the paper-based transaminase test for paired whole blood and serum specimens were then compared to the results of automated serum transaminase testing as the gold-standard (Fig. 5A–D). Given that EDTA plasma (separated from cells within 8 h of collection at room temperature) is an acceptable alternative specimen for testing by the automated assay used at BIDMC, it was assumed that gold standard results for the whole blood specimen (i.e. plasma) would have been equivalent to gold standard results for the paired serum specimen. Results for the single paper-based assay performed on each whole blood specimen (i.e. 3 results, one per reader) were averaged to generate each datum (Fig. 5B, D). For serum specimens, all specimens

with sufficient volume remaining after initial testing were stored at 4 °C and then blindly retested in triplicate (three readers blinded to the original automated results read each of three assays performed per specimen) within the subsequent 2.5 weeks and results of all tests performed on each serum specimen were then averaged to generate each datum (Fig. 5A, C) (unaveraged raw data are presented in Tables S1–S4). Internal studies at BIDMC have shown that automated serum transaminase results are stable in serum refrigerated for at least 2 weeks (data not shown); similarly, there was no systematic change in AST or ALT results in either direction (i.e. higher or lower) noted on repeat testing of stored serum specimens (data not shown).

Results of the paper-based assay for each specimen (paired whole blood and serum) were compared to the gold-standard serum transaminase results to evaluate “bin placement accuracy” (whether the result of the paper-based assay was in the same bin (<3x ULN, 3–5x ULN, or >5x ULN, as defined above) as the gold-standard result). The blue boxes (Fig. 5A-D) encompass values for which results of both the paper device and the gold-standard test were in the same bin. We calculated bin placement accuracy by determining if each datum met at least one of the following criteria: i) the value measured by the paper transaminase test was within the correct bin as determined by the automated (true) value, or ii) the value measured by the paper test was within 40 U/L of the true value (i.e. between the green and purple lines (Fig. 5A-D)). The second criterion accounted for values near the boundaries of the bins, as it was agreed that variations of <40 U/L near these boundaries were clinically acceptable as they were unlikely to reflect appreciable differences in clinical status, despite potentially changing management if strict cutoffs were to be used for decision-making (see Discussion). Results for the paper-based test that were neither within the correct bin nor within 40 U/L of the gold-standard result were considered inaccurate (red circles, Fig. 5A-D). It is important to note that samples below the

limits of detection (53 and 84 U/L for ALT and AST, respectively) would yield equivalent results from the colorimetric test. These threshold values are well within the <3x ULN range and no clinical action would be expected for the target patient population. Because the device is meant to detect substantially elevated (>3x ULN) transaminase levels, the assay chemistry is tailored to exhibit the greatest color changes between 3x and 5x ULN. Values well above 5x ULN, being out of the linear range, will appear the same on the test and will thus prompt the same clinical response (see also Discussion). Notably, the measuring range for the automated assay used at BIDMC is 4–400 U/L (0–10x ULN); higher values must be measured by sample dilution.

Bin placement accuracies are presented in Table 2. Overall accuracies for the device (data for all three bins in aggregate) were above 90% for both AST and ALT in both serum and whole blood. Additionally, “per bin” accuracies were calculated by dividing the number of correctly binned samples in each bin by the total number of samples in that bin. The data reveal that ALT accuracies were higher for serum than for whole blood, particularly in the 3–5x bin (92% vs 57%, respectively,  $p < 0.00003$ ). This disparity can be explained by the age of the whole blood (2–5 h, i.e. drawn from patient 2–5 h prior) at the time of testing. In early experiments (data not shown), we found that whole blood samples began to yield artificially high ALT values after aging for >3 h from the time of draw. We believe that this drift in values with age is due to the fact that, over time, red blood cells (RBCs) release lactate, which is then converted to pyruvate; the excess pyruvate leads to activation of the ALT assay and therefore falsely high readings. In the case of serum, RBCs are separated from the serum shortly after draw, preventing accumulation of pyruvate in serum. Therefore, accuracies from fresh whole blood (i.e. from a fingerstick) are expected to mirror the serum results in this study. This hypothesis has been

confirmed using freshly drawn whole blood samples with known amounts of ALT added (above), which do not generate falsely high results. Of note, this effect is not seen in commercial assays because these assays measure the kinetic rate of color formation after the native pyruvate is consumed during an initial incubation period.

We further evaluated device performance by Bland-Altman analysis (25). Specifically, we compared the semi-continuous data (reader estimates of actual values, to the nearest 10 U/L, obtained using the visual reading guide as described above) to the continuous data obtained by gold-standard automated testing. The goal of this analysis was to obtain a more highly resolved assessment of agreement with the gold-standard method, and to explore device bias and variability in the target clinical range (defined for this analysis as 40–250 U/L). The data (Fig. 6A-D) reveal several interesting points: i) A bias to overestimate the ALT whole blood data by 18 U/L on average is observed (Fig. 6B), likely due to pyruvate generation as described above. The 95% limits of agreement, the interval that we expect will contain 95% of paired differences, go from –63 U/L to +99 U/L for the ALT whole blood data set. ii) The AST whole blood (Fig. 6D) plot shows virtually zero bias and 95% limits of agreement from –59 to +62 U/L. iii) For serum ALT and AST values, we applied a log transformation to our data because the Bland-Altman plot of the untransformed data showed an increase in variability of the differences with increasing magnitude of measurement (Fig. S3). The log transformed Bland-Altman plots for ALT and AST serum successfully removed the relationship between differences and the mean (Fig. 6A, C). The data were then back-transformed to give values relating to the ratio of the untransformed measurements. Specifically, the paper-based test underestimated ALT serum by 9% on average and the 95% limits of agreement were between 60% lower and 90% higher for ALT serum. After the same transformation, AST serum results reveal that the paper-based test

overestimated AST serum by 12% on average and the 95% limits of agreement were between 63% lower and 100% higher.

As stated above, differences of  $\pm 40$  U/L are unlikely to change the course of treatment in many clinical situations. Moreover, the differences between color swatches on the read guide are each 20–30 U/L and we expect (though cannot easily quantify) that the maximum resolution of the device is similarly 20–30 U/L. We are therefore encouraged by these collective results as they suggest clinically acceptable agreement between the semi-quantitative paper test and the gold-standard automated assay method.

#### *Evaluation of analytes with potential for assay interference*

Studies were performed to assess common or known substances that could potentially interfere with ALT and AST assays. Our data suggest that pyruvic acid and ascorbic acid interfere with the ALT assay. Specifically, pyruvate present at levels  $>2$  mM may produce falsely elevated results in the ALT assay, and ascorbic acid present at levels  $>3$  mg/dL may produce falsely low ALT results. All of the other substances tested showed no marked interference in the ALT and AST assays at clinically relevant levels, including bilirubin ( $<10$  mg/dL), cholesterol ( $<500$  mg/dL), glucose ( $<1000$  mg/dL), lactate ( $<200$  mg/dL), urea ( $<100$  mg/dL), creatinine ( $<15$ mg/dL), and hemoglobin ( $<120$  mg/dL) (Methods). These results are consistent with our observations that the paper-based transaminase test performed well in the specimens from the clinically diverse population tested in this study (which included many patients who were critically ill with multi-organ failure and consequently multiple abnormal lab values (particularly bilirubin, lactate dehydrogenase, creatinine, and occasionally lipase)).

### *Assay Temperature and Read Time*

Fluctuations in temperature affect the speed of the test, most likely due to faster enzymatic reactions at higher temperatures (>30 °C). Our data indicate reliable performance of the paper-based transaminase test as performed at room temperature (22–30 °C) and read at 15 min. In the case of higher temperatures (31–37 °C), the test should be read at 10 min to obtain comparable results (data not shown).

### *Effects of blood volume on assay performance*

Different volumes (15, 20, 25, 30, 40, 50 µL) of blood, serum or buffer specimens with different AST/ALT concentrations were evaluated (data not shown). We did not observe that excess fluid altered the performance of the test, presumably because the paper device can only absorb a finite amount of fluid sample. Our data further show that at least 25–35 µL of sample is required for complete activation of the devices. This can be easily monitored in a field setting by adding blood until the filter is fully saturated (i.e. an all-red color is observed across the entire filter).

### *Assay Stability*

Stability of the paper transaminase test was evaluated by fabricating a single lot of devices and packaging them in heat-sealed, foil-lined pouches (10 tests per pouch) containing a silica desiccant packet. Pouches were stored at 25 °C and periodically opened to evaluate the devices using buffer standards (Methods). The results suggest that device performance, as measured by color intensity of the assays, did not vary by more than 8% after a period of 11 weeks at which point the study was concluded. This value is less than the %CV measured for the assays so the deviation can be attributed to device variability, not degradation. While this

timeframe is encouraging, devices may ultimately require two year stability to be viable products for the developing world. Future work will include thorough, long-term evaluations of device stability, including at elevated temperatures.

#### *Performance of the device in fingerstick testing*

We have conducted initial experiments to observe the performance of the device with whole blood obtained via fingerstick. In a small study, 10 healthy volunteers used a lancet (SurgiLance™ SLN300) to obtain a droplet (~30  $\mu$ L) of blood from a finger and introduced it to the device (Fig. 1B). 10/10 devices were found to fully activate, meaning that all zones were wet with plasma, and all controls worked properly. As expected, AST and ALT levels were found to be <60 U/L for all volunteers.



**Figures:**

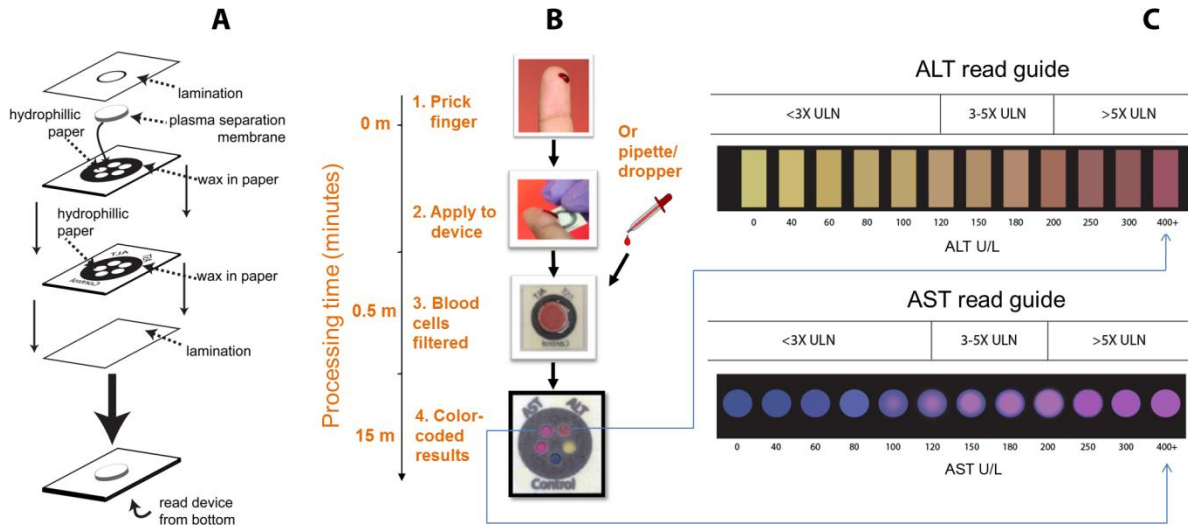


**Fig. 1.** Schema of the paper-based AST/ALT test design and protocol. **(A)** Device design (lamination layer, plasma separation membrane, layers of paper). **(B)** Use of the device. A drop of whole blood (either a fingerstick specimen or 30  $\mu$ L of a specimen obtained by venipuncture) is applied to the back of the device. Red and white blood cells are filtered out by the plasma separation membrane, while plasma wicks to the five detection zones via patterned hydrophobic channels in the paper. After 15 min, the AST (top left) and ALT (top right) test zones are matched to a color guide **(C)** to obtain a value in U/L. Results are interpreted as being within one of three “bins” of values: <3 times (3x) ULN (defined as 40 U/L); 3–5x ULN; or >5x ULN.

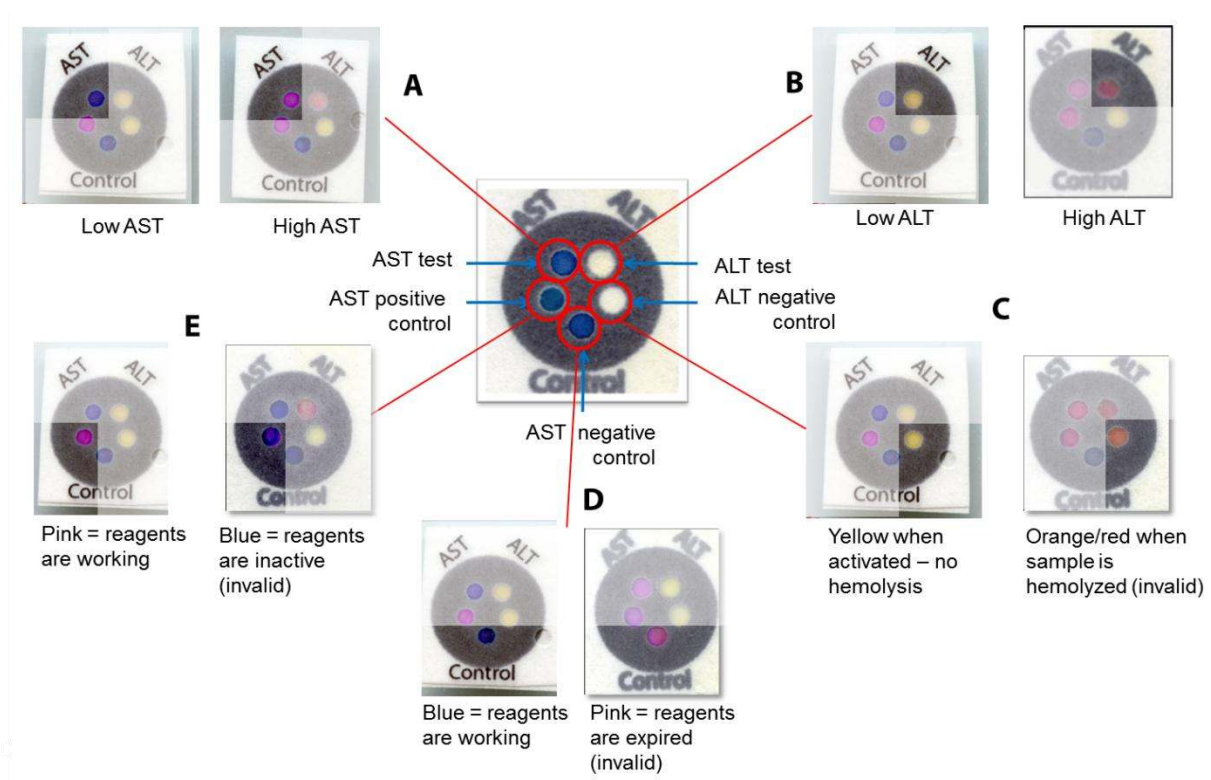


**Fig. 2.** Detailed schema of the paper-based transaminase test and possible readouts. A schematic of test and control zones (prior to receiving a sample) is shown in the center of the figure. **(A)** AST test zone: low/normal AST values (<80 U/L) result in a dark blue color (left panel), while high AST values (>200 U/L) result in a bright pink color (right panel). **(B)** ALT test zone: low/normal ALT values (<60 U/L) result in a yellow color (left panel), while high ALT values (>200 U/L) result in a deep red color (right panel). **(C)** ALT negative control zone: a change from white to yellow indicates appropriate device activation (complete wetting of the zone) (left panel); in the event of sample hemolysis, the zone becomes orange/red (right panel) and the device is read as “invalid.” **(D)** AST negative control zone: the baseline blue color remains unchanged if dye chemistry is functioning properly (left panel), while the zone becomes bright pink in the event of non-specific dye reaction (right panel) and the device is read as “invalid.” **(E)** AST positive control zone: the zone changes from blue to pink if AST reagents are

functioning properly (left panel), but remains dark blue if either the reagents are not functioning or the zone is not activated (right panel), and the device is read as “invalid.”

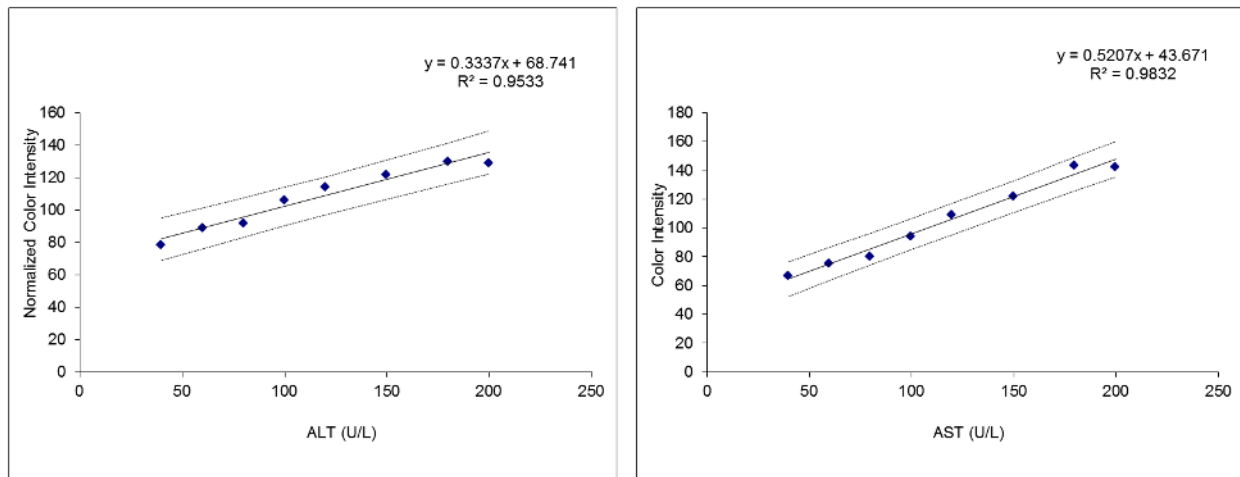


**Fig. 3.** Plot of color intensity versus concentration of ALT (left panel) or AST (right panel) in U/L. Each datum is an average of three measurements (i.e. three separate devices). Dashed lines represent the upper and lower 95% prediction intervals (Methods).

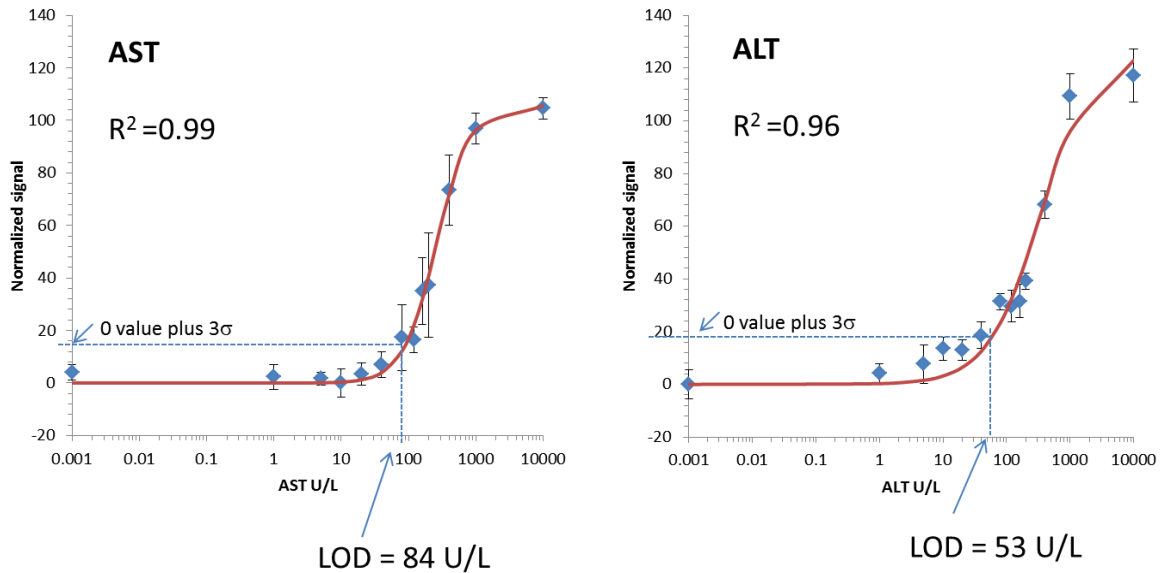


**Fig. 4.** Limits of detection curves for Aspartate aminotransferase (AST, left) and Alanine aminotransferase (ALT, right) using the paper-based transaminase test. Calibration plot of the output signal of the paper-based transaminase test versus the concentration of AST or ALT in the sample. For AST, the solid line represents a non-linear regression of Hill Equation:  $I = I_{\max}[L]^n / ([L]^n + [L_{50}]^n)$ , where  $I_{\max} = 105.7$ ,  $[L_{50}] = 260.9$  U/L,  $n = 1.72$ , and  $R^2 = 0.99$ . The error bars represent one standard deviation ( $\sigma$ ). For ALT, the solid line represents a non-linear regression of Hill Equation:  $I = I_{\max}[L]^n / ([L]^n + [L_{50}]^n)$ , where  $I_{\max} = 126.5$ ,  $[L_{50}] = 331.33$  U/L,  $n = 1.04$ , and  $R^2 = 0.96$ . The error bars represent one standard deviation ( $\sigma$ ). For both assays the linear portion of the sigmoidal curve ranges approximately within the concentrations of 40-200 U/L.

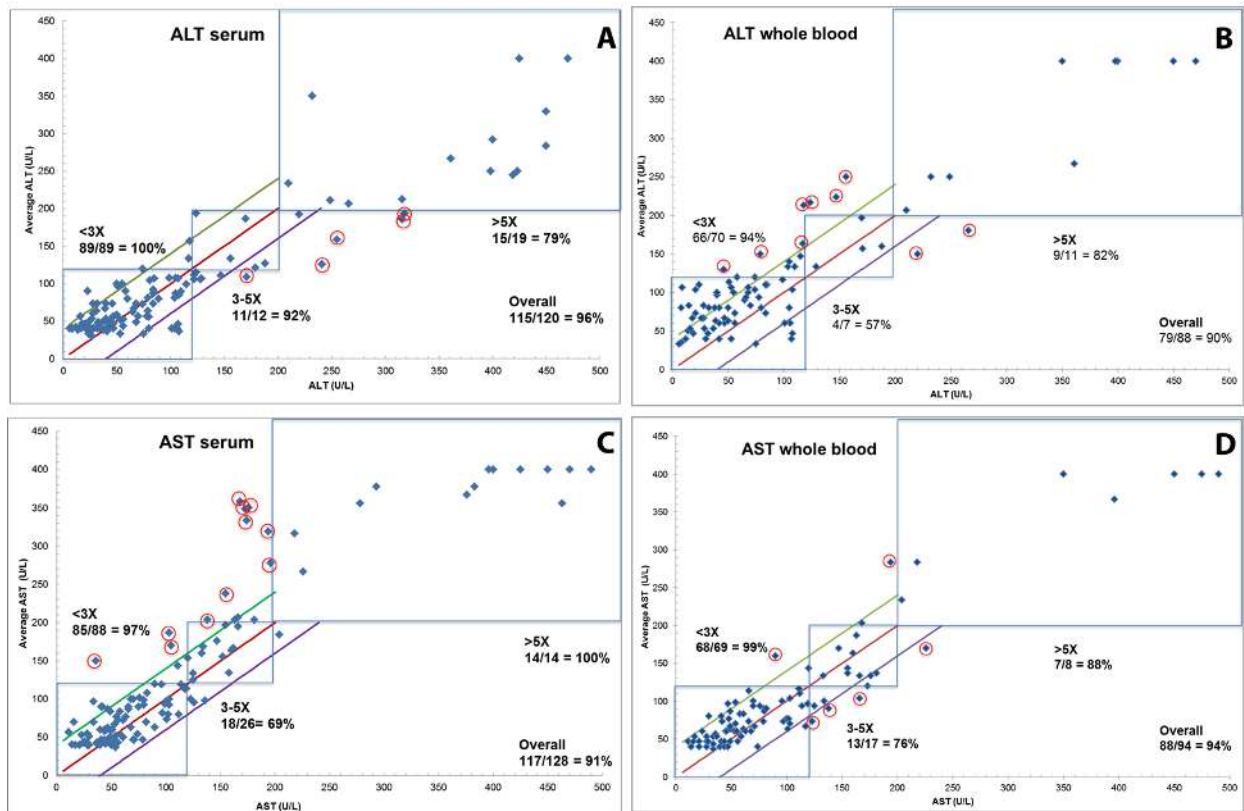


**Fig. 5.** Direct comparison of visual transaminase measurements made with the paper-based device to measurements made with a standard-of-care automated method. ALT (A, B) or AST (C, D) values in paired serum (A, C) or whole blood (B, D) clinical specimens are plotted against values (in U/L) measured in the serum specimen using a gold-standard automated method (Roche Modular Analytics System). In each plot, the blue boxes represent AST or ALT “bins” within which values for both the paper-based device and the automated method are within the same range, specifically <3X the ULN (0–119 U/L), 3–5X ULN (120–200 U/L), or >5X ULN (>200 U/L). The red line corresponds to the line of equality (paper device measurement = automated measurement) and the green and purple lines correspond to plus 40 U/L and minus 40 U/L from the line of equality, respectively. Points circled in red are samples that were neither in the correct bin nor within 40 U/L of the value measured by the gold-standard automated method

(see Results). For scaling purposes, X-axis values measured by the Roche system that exceeded 400 U/L were plotted between 400 and 500 U/L.

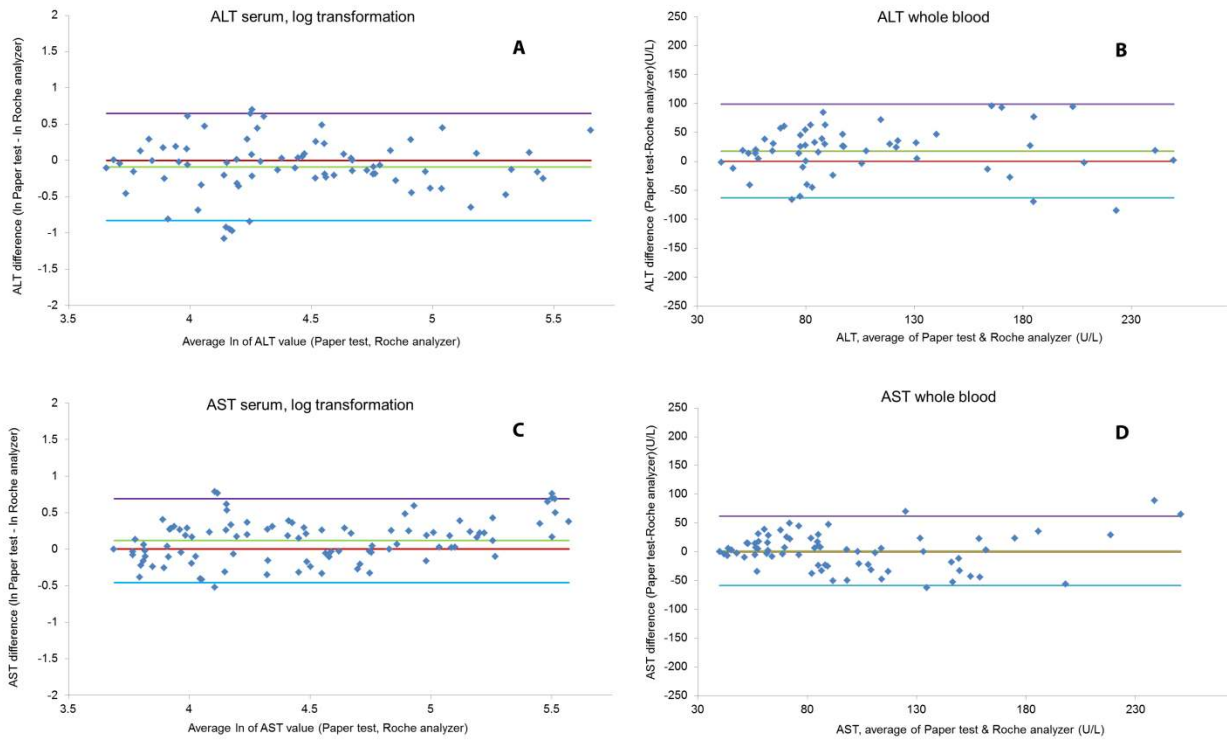


**Fig. 6.** Bland-Altman analysis of visual transaminase measurements in clinical specimens. **(A)** ALT values in serum (log transformation); **(B)** ALT values in whole blood; **(C)** AST values in serum (log transformation); **(D)** AST values in whole blood. The purple and blue lines represent the 95% limits of agreement (Methods). The red line is the line of equality and the green line is the average difference of the methods (Methods).

## Tables

		Serum Standard	Serum Standard	Whole Blood	Whole Blood
		Level 1 ALT= 56 U/L AST= 69 U/L	Level 2 ALT= 128 U/L AST= 244 U/L	Level 1 ALT= 40 U/L AST= 40 U/L	Level 2 ALT= 200 U/L AST= 200 U/L
<b>Alanine Aminotransferase (ALT)</b>	<b>Color Intensity Mean <math>\pm</math>S.D.</b>	111.0 $\pm$ 6.55	120.6 $\pm$ 11.2	93.6 $\pm$ 4.75	146.5 $\pm$ 10.59
	<b>%CV</b>	5.89	9.28	5.08	7.22
<b>Aspartate Aminotransferase (AST)</b>	<b>Color Intensity Mean <math>\pm</math>S.D.</b>	62.6 $\pm$ 5.52	151.1 $\pm$ 7.60	65.3 $\pm$ 5.24	168.5 $\pm$ 4.45
	<b>%CV</b>	8.82	5.03	8.01	2.64

**Table 1.** Repeatability of the paper transaminase test as measured by % coefficient of variation (CV). Samples were prepared as described (Methods) and each was tested with 10 devices. Color intensity was measured by scanning the devices using a desktop scanner and subsequently analyzing images of individual zones using ImageJ software (red and green channels were used for Aspartate aminotransferase (AST) and Alanine aminotransferase (ALT), respectively). %CV's were calculated by dividing the standard deviation by the mean intensity (N=10 devices per specimen with a given value).

Test	Specimen	Bin (X = 40 U/L = ULN)	No. of Samples in bin	No. Correctly Placed	“Per Bin ” Accuracy	Overall Accuracy
ALT	Serum	<3X	89	88	99%	95% (±4%)
		3–5X	12	11	92%	
		>5X	19	15	79%	
	Blood	<3X	70	66	94%	90% (±6%)
		3–5X	7	4	57%	
		>5X	11	9	82%	
AST	Serum	<3X	88	85	97%	91% (±5%)
		3–5X	26	18	69%	
		>5X	14	14	100%	
	Blood	<3X	69	68	99%	94% (±5%)
		3–5X	17	13	76%	
		>5X	8	7	88%	

**Table 2.** Bin placement accuracies for visual measurements in clinical specimens made using the paper-based transaminase test. 95% confidence intervals around the overall accuracy estimates are shown in parentheses.



## Discussion

We have demonstrated that we can accurately measure transaminases in whole blood and serum using a simple and very inexpensive paper-based assay that can be read by eye within minutes. Our test performed well, even in specimens that were obtained from critically ill patients with multiple derangements in other analytes, and that were up to 5h old at the time of testing. Variability, as measured by %CV, was found to be less than 10% for both assays using blood and serum samples. The experiments presented here have firmly established proof-of-concept and clinical relevance and will allow us to move into clinical field studies to evaluate the performance of our device in real time using fingerstick blood specimens from those patients for whom we see the device having highest utility, including those with TB, HIV, Hepatitis B, and Hepatitis C.

When sufficient resources are available, standard-of-care transaminase testing typically involves collecting a whole blood specimen by venipuncture, transporting the specimen to a central laboratory, centrifuging to separate serum, and testing the serum on a large automated platform. Such systems are impractically expensive for routine use in developing countries and require highly trained technicians for testing and maintenance. Moreover, the need to perform the testing in a central laboratory can considerably delay acquisition and dissemination of results, even if access to testing is available. In some resource-limited settings, it is not uncommon for tubes to get lost en route to the central laboratory, and transaminase results can sometimes take weeks or even months to return.

Manufacturing costs are dependent on several key variables, including location, making them difficult to calculate accurately a priori. We anticipate, however, that our device can ultimately be produced at a very low cost—on the order of a few pennies per test (Table S5). Two

FDA-approved devices do exist that could potentially be used for rapid POC testing, but, for both, utility for the resource-limited setting is limited by expense. The Roche Refletron Plus device requires venous blood draw, relies on complex electronics and electricity/battery, and is expensive (approximately \$6,000 for the reader and an additional \$4 per test.) Another device, the Cholestech LDX, is capable of using fingerstick samples, but the reader and tests are similarly expensive (approximately \$3,000/\$4, respectively).

Our test has been optimized for detection of AST and ALT values  $>3x$  ULN, in light of guidelines (e.g. for TB treatment (*1*)) that place great emphasis on the  $3x$  ULN and  $5x$  ULN cutoffs (in concert with symptoms of hepatotoxicity) for making management decisions. While we hope to have sufficient resolution in the  $3-5x$  range to allow highly accurate bin placement, we also believe that our test could have great benefit as a “rule-out” or “triage” test. Specifically, if AST or ALT was observed to be  $<3x$  ULN on routine screening with the POC test, no further testing would be indicated; if values on the POC test were  $>3x$  ULN, the patient could proceed to quantitative testing by venipuncture/automated method. Such use would save valuable clinical resources and time, while still making triage testing available in remote areas. The work presented here indicates that our bin placement accuracies for the  $<3x$  ULN bin are near 100%. Our results for ALT (whole blood) indicate that no specimens with gold-standard ALT values  $>120$  U/L were read by the paper-based test as  $<120$  U/L (Fig. 5B). For AST (whole blood), a small number of samples with gold-standard AST values  $>120$  U/L were read by the paper-based test as  $<120$  U/L (Fig. 5D), and this is a focus of current experiments. Importantly, there were no specimens that had gold-standard AST or ALT values  $>5x$  ULN and were read as  $<3x$  ULN (Fig. 5) (TB treatment guidelines (*1*), for example, recommend that patients with

levels >5x ULN stop their TB medications, even if asymptomatic). Performance of the device at the 3x ULN cutoff will be closely examined as we move into real-time fingerstick testing.

We are currently working on a number of enhancements to the test, which include: i) a telemedicine application whereby the colorimetric results of the test could be recognized and quantified via smartphone (facilitating increased resolution of results and ease of results documentation/transmission, and obviating any concerns about color-blind users); ii) the addition of other zones/features to indicate proper device performance and enhance user interaction, and iii) large-scale manufacturing methods and techniques, such as robotic spotting of reagents, to improve throughput and precision.

Hepatotoxicity is a major adverse event associated with both anti-tuberculous and anti-retroviral therapy, and monitoring for drug-induced liver injury (DILI) is accordingly a major priority in the care of these patients. Moreover, there are other important and common global conditions (such as epilepsy) for which treatment can be associated with substantial hepatotoxicity. We anticipate that our device will dramatically simplify and reduce the cost of detection and monitoring progression of DILI, making extremely inexpensive, minimally invasive, and accurate transaminase testing available at POC for all who need it and thus providing distinct advantages over standard-of-care automated methods using venipuncture. Conceivably, our fingerstick test could also improve treatment adherence (9). Finally, successful development of this novel platform will facilitate the development of similar novel POC clinical assays for monitoring other clinically important analytes.

## Materials and Methods

### *Device fabrication*

Device patterns were designed using Adobe Illustrator CS3. The pattern consisted of 12 rows of 9 devices for a total of 108 devices per sheet (Fig. S2). Whatman No. 1 chromatography paper (8.5x11") was fed into a laser printer (HP Color Laserjet 4520) and nine 0.85x14 cm yellow (Y=100% on CMYK scale) stripes were printed on the sheet. A wax pattern (Fig. S2) for the top layer (layer from which the device is read) was printed onto this sheet using a Xerox 8560DN printer such that the wax pattern was printed on the opposite side of the paper as the yellow stripe and that the yellow stripes only covered the back face of the ALT test zones and ALT negative controls in each column (i.e. did not cover the back face of the AST test or AST control zones). The sheet was heated in a gravity convection oven at 150 °C for 30 s. A wax pattern for the bottom layer (layer in contact with filters) was printed onto Whatman No. 1 Chromatography paper using a Xerox 8560DN printer and heated in the oven at 150 °C for 30 s. This layer did not have a yellow stripe on the reverse side of the paper. A pressure-sensitive adhesive (UNITAK 131, Henkel) was applied to the back of the top layer by screen printing such that the 5 active zones of the device did not receive adhesive but the remaining areas did. The layer was placed in a gravity convection oven set to 70 °C for 15 min. This screen-printing and heating process was repeated on the back of the bottom layer. The sheets were then taped to a plastic frame in order to spot reagents. Details of the reagents used in each zone (ALT and AST test zones, and three control zones) are provided in Supplementary Methods; zones were spotted using a micropipette according to Fig. S1. Where multiple reagent spots were required (ALT test zone, AST positive control zone), the first spot was allowed to dry completely (air dry at room temperature) before applying the second. A hole-puncher was used to punch alignment holes

(preprinted on the corners of each sheet) in both device layers. The layers were aligned and laminated using a benchtop laminator (Apache AL13P) at a speed of 2 ft/min. Cold lamination (Fellowes self-adhesive laminate sheets) was then placed on the front face of the sheet of devices. An array consisting of 108 holes (each hole aligned with the center of a device), each with a diameter of 7mm was cut on a second sheet of laminate using a knife plotter (Craftrobo Silhouette CC330L-20 SD) and placed on a bench adhesive side up. 1 cm pre-cut discs of Pall Vivid GX plasma separation membrane were then centered over the holes in the laminate sheet in such a way that the rough side of the membrane was in contact with the adhesive. The cut laminate with adhered filters was then aligned and laminated to the back of the device sheet stack such that each filter covered all 5 zones of the device. Finally, the entire stack was laminated to ensure good contact between all layers. Individual devices were then cut by hand and stored in heat-sealed foil-lined bags containing 1 packet of silica desiccant (Sigma) with 10 devices / bag.

### *Read Guide*

The read guide (Fig. 1C) was generated by adding known amounts (as provided by the vendor) of AST and ALT (Lee bio) to fresh whole blood (drawn by venipuncture, baseline AST/ALT 24/22 U/L) to generate final concentrations of 40, 60, 80, 100, 120, 150, 180, 200, 250, 300, and 400 U/L. 30  $\mu$ L of sample were added to each of 3 devices for all concentrations. After 15 min, the devices were scanned using a desktop scanner (Canon). Experiments were performed at room temperature (25 °C). Images were analyzed using Adobe Illustrator CS3 to generate color swatches with the appropriate CMYK values. The read guide was printed and laminated between two Fellowes self-adhesive laminate sheets using a benchtop laminator (Apache AL13P).

### *Linearity Studies*

For linearity studies, measured amounts of AST and ALT (Lee Bio) were added to fresh whole blood (drawn by venipuncture, baseline AST/ALT 24/22 U/L) to generate final concentrations of 40, 60, 80, 100, 120, 150, 180, 200, 250, 300, and 400 U/L. 30  $\mu$ L of sample were added to each of 3 devices for all concentrations. After 15 minutes, the devices were scanned using a desktop scanner (Canon). Experiments were performed at room temperature (25 °C). Images were analyzed using ImageJ software (NIH) to obtain color intensity values for each zone. ALT data were quantified using the green channel and final values were normalized by subtracting from 255 (255 is the maximum color intensity value in the RGB color model and this normalization allows for a positive correlation between ALT values and color intensity in the green channel). AST data were quantified using the red channel without normalization. 95% prediction intervals were calculated using an excel macro, PredInt.xls, version 8.3.

### *Limit of Detection Studies*

For limit of detection studies, measured amounts of AST and ALT (Lee Bio) were added to artificial blood plasma buffer to generate final concentrations of 0.1, 1, 5, 10, 20, 40, 80, 120, 160, 200, 400, 1000, and 10,000 U/L. 30  $\mu$ L of sample were added to each of 7 devices for all concentrations. After 15 minutes, the devices were scanned using a desktop scanner (Canon). Experiments were performed at room temperature (25 °C). Images were analyzed using ImageJ software (NIH) to obtain color intensity values for each zone. ALT data were quantified using the green channel and final values were normalized by subtracting from 255. AST data were quantified using the red channel without normalization.

### *Repeatability Studies*

For repeatability studies, commercial serum standards containing known (as measured by the vendor) AST/ALT values were purchased from Pointe Scientific. Two levels were used for these studies: Level I standards contained 69/56 U/L of AST/ALT respectively and Level II standards contained 244/128 U/L of AST/ALT respectively. Whole blood samples were also prepared by adding known amounts of AST and ALT (Lee Bio) to fresh whole blood (drawn by venipuncture, baseline AST/ALT 24/22 U/L) to generate final concentrations of 40 (Level I) and 200 U/L (Level II). A total of four samples were prepared for testing (Level I/II serum samples and Level I/II whole blood samples). 30  $\mu$ L of sample were added to each of 10 devices for all concentrations. Experiments were performed at room temperature (25 °C). After 15 minutes, the devices were scanned using a desktop scanner (Canon). Images were analyzed using ImageJ software (NIH) to obtain color intensity values for each zone. ALT data were quantified using the green channel and final values were normalized by subtracting from 255. AST data were quantified using the red channel without normalization.

### *Stability Studies*

For stability studies, approximately 100 devices were fabricated and stored in foil-lined pouches (Plastic Bags For You), 10 tests to a pouch, each containing 1 packet of silica desiccant (Sigma). The pouches were sealed using a Hualian heat sealer. The pouches were stored at 25°C and were tested at 0, 4, 8, 14, 21, 33, 42, 63, and 77 days using buffer standards prepared in artificial blood plasma buffer. Buffer standards were generated by adding measured amounts of AST and ALT (Lee bio) to artificial blood plasma buffer to generate final concentrations of 40 and 200 U/L. 30  $\mu$ L of sample were added to each device for all concentrations. After 15

minutes, the devices were scanned using a desktop scanner (Canon). Experiments were performed at room temperature (25 °C). Images were analyzed using ImageJ software (NIH) to obtain color intensity values for each zone. ALT data were quantified using the green channel and final values were normalized by subtracting from 255. AST data were quantified using the red channel without normalization.

#### *Experiments to evaluate potential interfering factors*

Human serum samples with baseline AST/ALT levels measured by the supplier were obtained from Valley Biomedicals Inc. Purified ALT/AST (Lee bio) was then added to generate final levels of approximately 40 U/L (normal, representing 1-3X ULN bin), 150 U/L (elevated, representing 3-5X ULN bin) and 400 U/L (highly elevated, representing >5X ULN bin). Stock solutions of potential interfering reagents were prepared and added to the above three types of ALT/AST serum samples at different final concentrations.

#### *Collection and testing of clinical specimens*

The protocol for access to discarded clinical specimens and associated clinical data was approved by the Investigational Review Board of Beth Israel Deaconess Medical Center (BIDMC). Routine clinical transaminase testing (AST/ALT) at BIDMC was performed on serum specimens by the BIDMC clinical chemistry laboratory using a Roche Modular Analytics System (P800 spectrophotometer module). Paired whole blood (drawn in lavender-top EDTA tube) and serum (drawn in green-top heparin serum separator tube) specimens that were less than 5 hours old (age defined as time since venipuncture) were identified by searching electronically for reported serum AST and ALT results that spanned the clinical range and then confirming that a whole blood specimen had been drawn from that patient at the same time. 200 microliter aliquots of



each specimen were removed and these aliquots were de-identified. 30 microliter aliquots of each de-identified specimen were applied to individual devices by micropipette. 15 minutes after application, results were read by eye in silence by three independent readers who were blinded to the results of automated transaminase testing of the serum specimens. Results were interpreted by comparing color changes in the ALT and AST test zones to the read guide (Fig. 1C) and results were recorded as values rounded to the nearest 10 U/L. Control zone colors were checked according to Fig. 2 to confirm proper device function. Whole blood specimens were discarded after initial testing; serum specimens were stored at 4 °C for repeat testing (Results). Fingerstick specimens were obtained from volunteers at Diagnostics For All, all of whom provided verbal consent after hearing a detailed explanation of the test procedure.

#### *Bland-Altman Analysis*

Bland-Altman analysis was conducted for values ranging from 0-275 U/L for each data set (ALT whole blood, ALT serum, AST whole blood, AST serum). Values greater than 275 U/L were removed from this analysis because the test signal saturates above this threshold. Such values resulted in artificially high 95% limits of agreement. Furthermore, the clinical action is the same for all values in this bin. For example, a value of 2000 U/L (as measured by the Roche instrument) would saturate the paper test signal and yield a visual value of 400 U/L. The D value (defined below) for this data point would be -1600 U/L despite correctly identifying the sample in the >5X ULN bin.

Bland-Altman analysis was conducted by calculating the following:

$$D_i = (P_i - R_i)$$

Where  $D_i$  is the difference between a value measured by the Paper transaminase test ( $P_i$ ) and the Gold-Standard Roche Instrument ( $R_i$ ). A scatter plot was generated using Microsoft Excel consisting of  $(M_i, D_i)$  for each data point in the series where  $M_i$  is the average of  $P_i$  and  $R_i$ .

The mean difference ( $U$ ) was calculated according to the following equation:

$$U = \frac{1}{n} \sum_{i=1}^n D_i$$

Where  $U$  is the average difference,  $D_i$  is the difference between the methods for a given point and  $n$  is the number of samples.  $U$  was then plotted as a straight line on the scatter plot as the equation  $Y=U$ . The standard deviation ( $S_d$ ) of  $D_i$  was calculated according to the following equation:

$$S_d = \sqrt{\frac{1}{n} \sum_{i=1}^n (D_i - U)^2}$$

95% limits of agreement were calculated according to the equations:

$L_1 = U + (1.96)S_d$  where  $L_1$  is the upper limit of agreement,  $U$  is the mean difference and  $S_d$  is the standard deviation of  $D_i$ .  $L_2 = U - (1.96)S_d$  where  $L_2$  is the lower limit of agreement,  $U$  is the mean difference and  $S_d$  is the standard deviation of  $D_i$ .  $L_1$  and  $L_2$  were then plotted as straight lines on the scatter plot as the equations  $Y=L_1$  and  $Y=L_2$ . The line of equality was plotted as straight line according to the equation ( $Y=0$ )

Log transformation was applied according to the methods described by Bland and Altman (18). Briefly, Y axis values were obtained by taking the natural logarithm (Ln) of the Paper test and Roche values and subtracting Ln Roche from Ln Paper test. X axis values were obtained by averaging Ln Paper test and Ln Roche values. 95% limits of agreement were calculated as described above only using the log transformed values. Limits of agreement were then back transformed with an antilog function ( $e^x$ ).

## **Supplementary Materials**

Materials and Methods - Reagents for ALT assay, Regents for AST assay

Fig. S1. Locations of spotted reagent solutions for ALT and AST assays.

Fig. S2. Device pattern generated in Adobe Illustrator used for wax printing of device sheets on paper.

Fig. S3. Bland-Altman analysis of visual transaminase measurements in clinical serum specimens prior to the log transformation done for Figure 5.

Table S1. ALT whole blood raw data

Table S2. AST whole blood raw data

Table S3. ALT serum raw data

Table S4. AST serum raw data

Table S5. Cost per device estimate of the paper-based transaminase test

## References:

1. J. J. Saukkonen, D. L. Cohn, R. M. Jasmer, S. Schenker, J. A. Jereb, C. M. Nolan, C. A. Peloquin, F. M. Gordin, D. Nunes, D. B. Strader, J. Bernardo, R. Venkataramanan, T. R. Sterling, An official ATS statement: hepatotoxicity of antituberculosis therapy. *Am. J Respir. Crit. Care Med.* **174**, 935-952 (2006).
2. Panel on Antiretroviral Guidelines for Adults and Adolescents. Guidelines for the use of antiretroviral agents in HIV-1-infected adults and adolescents. *Department of Health and Human Services.*, 1-161. Available at <http://www.aidsinfo.nih.gov/ContentFiles/AdultandAdolescentGL.pdf>.
3. A. Tostmann, M. J. Boeree, R. E. Aarnoutse, W. C. de Lange, A. J. van der Ven, R. Dekhuijzen, Antituberculosis drug-induced hepatotoxicity: concise up-to-date review. *J. Gastroenterol. Hepatol.* **23**, 192-202 (2008).
4. J. M. McKoy, C. L. Bennett, M. H. Scheetz, V. Differding, K. L. Chandler, K. K. Scarsi, P. R. Yarnold, S. Sutton, F. Palella, S. Johnson, E. Obadina, D. W. Raisch, J. P. Parada, Hepatotoxicity associated with long- versus short-course HIV-prophylactic nevirapine use: a systematic review and meta-analysis from the Research on Adverse Drug events And Reports (RADAR) project. *Drug Saf.* **32**, 147-158 (2009).
5. E. Martinez, J. L. Blanco, J. A. Arnaiz, J. B. Perez-Cuevas, A. Mocroft, A. Cruceta, M. A. Marcos, A. Milinkovic, M. A. Garcia-Viejo, J. Mallolas, X. Carne, A. Phillips, J. M. Gatell, Hepatotoxicity in HIV-1-infected patients receiving nevirapine-containing antiretroviral therapy. *AIDS.* **15**, 1261-1268 (2001).
6. L. K. Shipton, C. W. Wester, S. Stock, N. Ndwapi, T. Gaolathe, I. Thior, A. Avalos, H. J. Moffat, J. J. Mboya, E. Widenfelt, M. Essex, M. D. Hughes, R. L. Shapiro, Safety and

- efficacy of nevirapine- and efavirenz-based antiretroviral treatment in adults treated for TB-HIV co-infection in Botswana. *Int. J. Tuberc. Lung. Dis.* **13**, 360-366 (2009).
7. C. J. Hoffmann, S. Charalambous, C. L. Thio, D. J. Martin, L. Pemba, K. L. Fielding, G. J. Churchyard, R. E. Chaisson, A. D. Grant, Hepatotoxicity in an African antiretroviral therapy cohort: the effect of tuberculosis and hepatitis B. *AIDS.* **21**, 1301-1308 (2007).
  8. Severe isoniazid-associated liver injuries among persons being treated for latent tuberculosis infection --- United States, 2004--2008. *MMWR Morb. Mortal. Wkly. Rep.* **59**, 224-229.
  9. F. K. Shieh, G. Snyder, C. R. Horsburgh, J. Bernardo, C. Murphy, J. J. Saukkonen, Predicting non-completion of treatment for latent tuberculous infection: a prospective survey. *Am. J. Respir. Crit. Care Med.* **174**, 717-721 (2006).
  10. A. W. Martinez, S. T. Phillips, G. M. Whitesides, E. Carrilho, Diagnostics for the developing world: microfluidic paper-based analytical devices. *Anal. Chem.* **82**, 3-10 (2010).
  11. A. W. Martinez, S. T. Phillips, E. Carrilho, S. W. Thomas, 3rd, H. Sindi, G. M. Whitesides, Simple telemedicine for developing regions: camera phones and paper-based microfluidic devices for real-time, off-site diagnosis. *Anal. Chem.* **80**, 3699-3707 (2008).
  12. A. W. Martinez, S. T. Phillips, M. J. Butte, G. M. Whitesides, Patterned paper as a platform for inexpensive, low-volume, portable bioassays. *Angew. Chem. Int. Ed. Engl.* **46**, 1318-1320 (2007).
  13. A. W. Martinez, S. T. Phillips, G. M. Whitesides, Three-dimensional microfluidic devices fabricated in layered paper and tape. *Proc. Natl. Acad. Sci. U S A* **105**, 19606-19611 (2008).
  14. C. M. Cheng, A. W. Martinez, J. Gong, C. R. Mace, S. T. Phillips, E. Carrilho, K. A. Mirica, G. M. Whitesides, Paper-based ELISA. *Angew. Chem. Int. Ed. Engl.* **49**, 4771-4774 (2010).

15. Z. Nie, F. Deiss, X. Liu, O. Akbulut, G. M. Whitesides, Integration of paper-based microfluidic devices with commercial electrochemical readers. *Lab. Chip.* **10**, 3163-3169 (2010).
16. J. L. Osborn, B. Lutz, E. Fu, P. Kauffman, D. Y. Stevens, P. Yager, Microfluidics without pumps: reinventing the T-sensor and H-filter in paper networks. *Lab. Chip.* **10**, 2659-2665 (2010).
17. E. Fu, B. Lutz, P. Kauffman, P. Yager, Controlled reagent transport in disposable 2D paper networks. *Lab. Chip.* **10**, 918-920 (2010).
18. B. R. Lutz, P. Trinh, C. Ball, E. Fu, P. Yager, Two-dimensional paper networks: programmable fluidic disconnects for multi-step processes in shaped paper. *Lab. Chip.* **11**, 4274-4278 (2011).
19. E. Fu, P. Kauffman, B. Lutz, P. Yager, Chemical signal amplification in two-dimensional paper networks. *Sens. Actuators. B. Chem.* **149**, 325-328 (2010).
20. M. S. Khan, G. Thouas, W. Shen, G. Whyte, G. Garnier, Paper diagnostic for instantaneous blood typing. *Anal. Chem.* **82**, 4158-4164 (2010).
21. X. Li, J. Tian, G. Garnier, W. Shen, Fabrication of paper-based microfluidic sensors by printing. *Colloids Surf. B. Biointerfaces.* **76**, 564-570 (2010).
22. W. Dungchai, O. Chailapakul, C. S. Henry, Use of multiple colorimetric indicators for paper-based microfluidic devices. *Anal. Chim. Acta.* **674**, 227-233 (2010).
23. E. M. Fenton, M. R. Mascarenas, G. P. Lopez, S. S. Sibbett, Multiplex lateral-flow test strips fabricated by two-dimensional shaping. *ACS Appl. Mater. Interfaces.* **1**, 124-129 (2009).
24. S. J. Vella, R. Cademartiri, A. Laromaine, P.D. Beattie, A.W. Martinez, S.T. Phillips, K.A. Mirica, G.M. Whitesides, Measuring Markers of Liver Function Using a Micro-Patterned

Paper Device Designed for Blood from a Fingerstick. *Anal. Chem.*, (Published online Feb. 12, 2012).

25. J. M. Bland, D. G. Altman, Measuring agreement in method comparison studies. *Stat. Methods. Med. Res.* **8**, 135-160 (1999).

**Acknowledgments:** We thank the staff of the BIDMC clinical chemistry lab, particularly Manuel Alves, Wayne Rhymer, and Anders Berg, for their guidance and assistance regarding collection of discarded specimens. We also thank Obsidiana Abril-Hörpel, Bill Haag, and Ann Pierson for helpful discussions. **Funding:** This work was supported in part by a grant from the Department of Defense Center for Integration of Medicine and Innovative Technology (CIMIT)(W81XWH-09-2-0001). N.P. is supported by a National Institute of Health K23 grant (1 K23 AI074638-01A2). J.R., S.K., P.B., S.J., and U.R. are supported by a Harvard subcontract of a grant from the Bill & Melinda Gates Foundation (51308 – Zero Cost Diagnostics). **Author Contributions:** J.R., S.K., and P.B designed the device. N.P., J.R., S. K., S.J. and P.B. designed and conducted the studies and designed/optimized test readout. S.J. performed device fabrication and assisted in device optimization studies. R.P. assisted with discarded specimen collection and analysis. V.W. conducted the limit of detection studies. N.P., J.R., S.J. and S.K. analyzed data; F.N. advised on data analysis; N.P. and J.R. wrote the paper; all co-authors edited the paper. U. R. and G.W. advised on approach and overall scope. **Competing Interests:** Patent application filed pertaining to results: U.S. Provisional Patent Application No. 61/555,977 "Quantitative Microfluidic Devices" by Rolland *et al.*

## **Supplementary Methods:**

### *Reagents for ALT Assay*

**Alanine Solution** - A solution containing 1M L-alanine (Sigma Aldrich), 30 mM  $\alpha$ -ketoglutaric acid (Sigma Aldrich), 2 mM  $\text{KH}_2\text{PO}_4$ (Sigma Aldrich), 20 mM  $\text{MgCl}_2$  (Sigma Aldrich), 2 mM Thiamine Pyrophosphate (MP Biosciences), 2 mM of 4-aminoantipyrine (Sigma Aldrich) and 25 U/mL (0.1 mg/mL) Horseradish Peroxidase (HRP) (Sigma Aldrich) was prepared in 200 mM Tris buffer (pH=7.4).

**DABA Solution** – A solution containing 10 wt% PEG (MW = 35,000 g/mol, Sigma Aldrich) and 10 mM Dimethylaminobenzoic acid was prepared in DI water.

**Pyruvate Oxidase** – A solution containing 100 U/mL of Pyruvate Oxidase (MP Biosciences, EMD) was prepared in 200mM Tris buffer pH=7.4.

**PEG Solution** - A solution containing 5wt% PEG (MW = 35,000 g/mol, Sigma Aldrich) was prepared in DI water.

### *Reagents for AST Assay*

**AST Dye Solution**- A solution containing 0.5% Methyl Green, 0.05% Rhodamine B, 0.025% Triton X 100, 1% PVA (13,000-23,000 g/mol) was prepared in DI water.

**CSA Solution** – A solution containing 171.1 mg CSA (Sigma Aldrich), 14.6 mg  $\alpha$ -ketoglutaric acid and 10 $\mu$ L of 200mM EDTA solution was prepared in 1 mL of 40 mM Phosphate Buffer and the pH was adjusted to 8.0.



**AST Positive Control Solution (200KU/L AST solution, 5% PEG, in 1X PBS)** – A solution was prepared containing 5% PEG (MW = 35,000 g/mol, Sigma Aldrich) in 1X PBS and 6.17  $\mu\text{L}$  AST (5177 U/mL, MP Biosciences) were added to make 200 kU/L AST solution.

**Artificial Blood Plasma Buffer** – A solution containing 84% NaCl, 4%  $\text{NaHCO}_3$ , 2% KCl, 2%  $\text{Na}_2\text{HPO}_4 \cdot 3\text{H}_2\text{O}$ , 3%  $\text{MgCl}_2 \cdot 6\text{H}_2\text{O}$ , 3%  $\text{CaCl}_2$ , 1%  $\text{Na}_2\text{SO}_4$  was prepared in DI water and the pH was adjusted to 7.4.

**Supplementary Figures:**

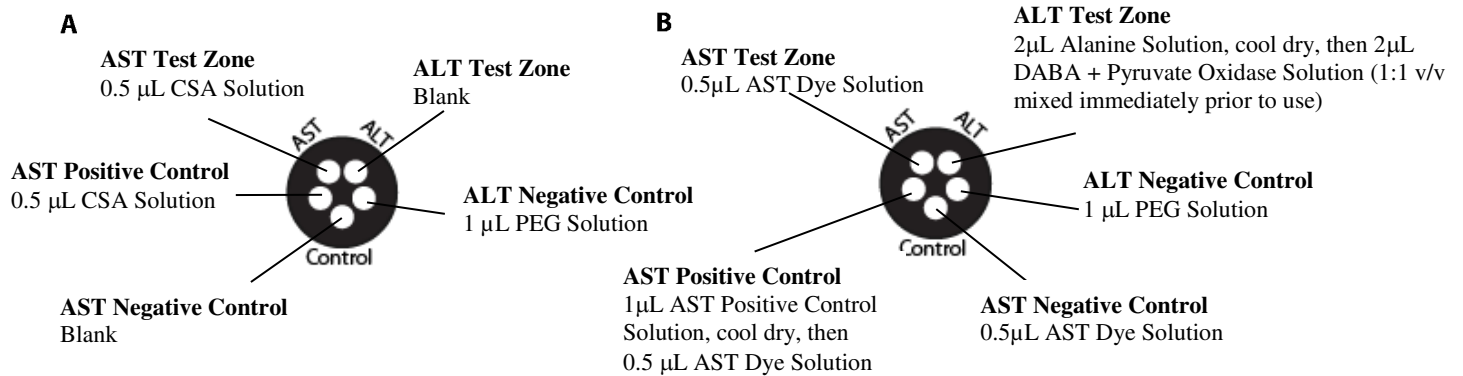


**Fig. S1.** Locations of spotted reagent solutions for ALT and AST assays. Two layers of patterned paper are used in the paper transaminase test, one in which the back side is directly in contact with the filter membrane (**A**), and one from which the results are read (**B**).

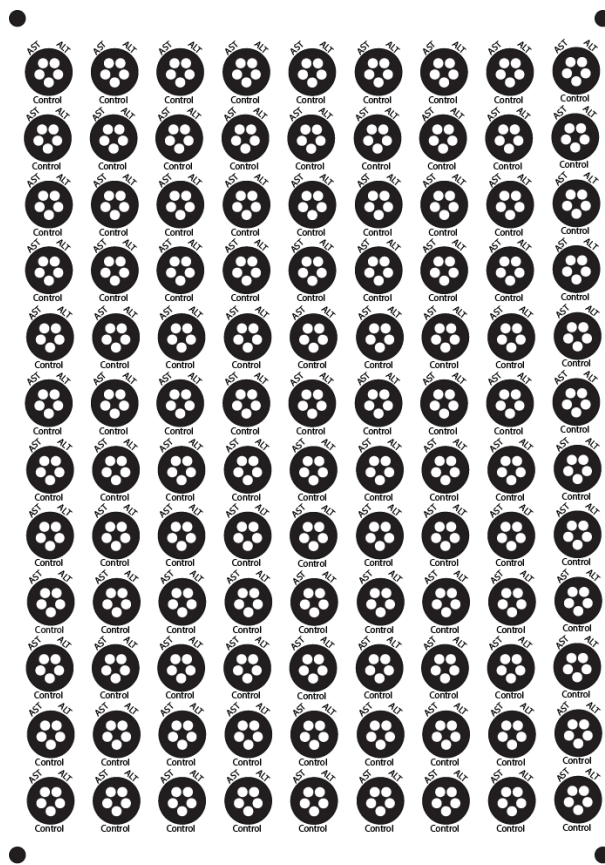


**Fig. S2.** Device pattern generated in Adobe Illustrator used for wax printing of device sheets on paper.

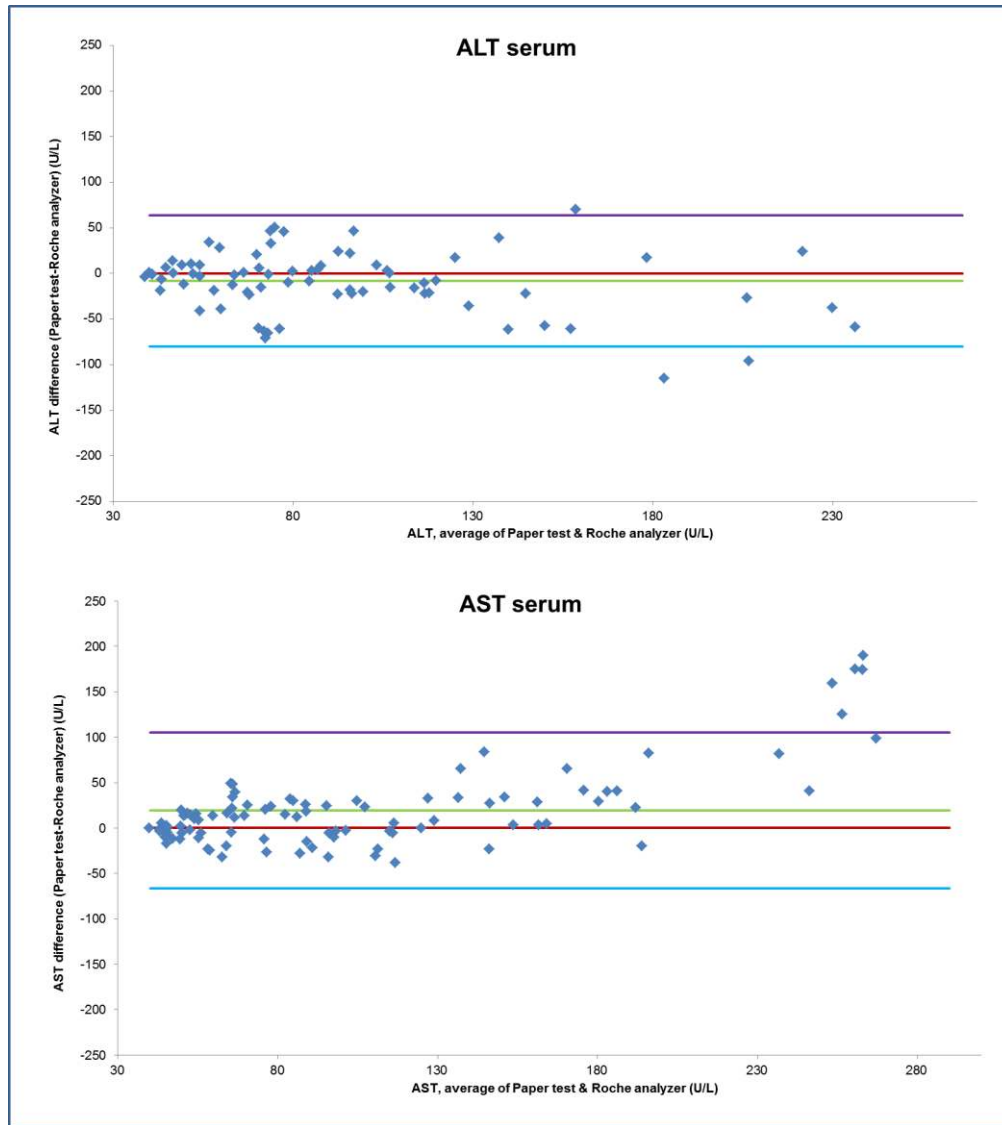


**Fig. S3.** Bland-Altman analysis of visual transaminase measurements in clinical serum specimens prior to the log transformation done for Fig. 6. Alanine aminotransferase (ALT) and Aspartate aminotransferase (AST) levels were measured in serum specimens with the paper-based device, and compared to ALT/AST results measured in the serum specimens by a gold-standard automated method (Roche, Methods). For each of the data points shown, the difference between ALT or AST levels measured by the two methods was plotted on the y axis, vs the average value of the two methods on the x axis. ALT values in serum (top); AST values in serum (bottom). The purple and blue lines represent the 95% limits of agreement (Methods). The red line is the line of equality and the green line is the average difference of the methods (Methods).

**Supplementary Tables:**

<b>Roche Analyzer Value (U/L)</b>	<b>Paper Test Value Reader 1 (U/L)</b>	<b>Paper Test Value Reader 2 (U/L)</b>	<b>Paper Test Value Reader 3 (U/L)</b>	<b>Paper Test Value Average (U/L)</b>
6	40	40	20	33
8	40	40	25	35
8	80	80	80	80
9	100	110	110	107
12	40	40	40	40
14	50	60	40	50
15	90	70	90	83
16	60	40	60	53
17	50	60	40	50
18	60	80	60	67
19	40	40	60	47
21	80	60	80	73
21	100	100	110	103
24	100	120	110	110
26	60	60	80	67
28	60	60	80	67
28	70	100	80	83
29	60	40	60	53
30	40	40	40	40
32	40	40	60	47
33	80	60	100	80
37	60	40	60	53
38	80	80	80	80
39	70	40	80	63
40	80	100	110	97
40	100	100	100	100
42	40	20	60	40
42	60	40	80	60
42	80	80	80	80
46	120	120	150	130
47	60	60	60	60
47	60	80	60	67
50	60	50	80	63
50	100	80	60	80
51	120	100	120	113
53	40	40	40	40
53	110	110	100	107
55	100	90	110	100
56	60	40	80	60
56	60	80	80	73
58	120	110	130	120
65	80	80	110	90
66	100	80	100	93

68	100	100	100	100
68	120	100	100	107
70	80	80	90	83
74	100	100	110	103
74	100	120	140	120
75	40	20	40	33
78	100	80	100	93
79	150	150	150	150
80	60	80	100	80
84	60	60	100	73
84	110	120	100	110
85	100	110	120	110
99	120	100	130	117
101	60	60	60	60
104	120	120	160	133
105	60	70	110	80
105	130	130	160	140
106	60	60	60	60
107	40	40	40	40
108	40	40	60	47
108	100	100	110	103
110	130	120	150	133
115	150	160	130	147
117	150	160	180	163
118	200	250	190	213
124	250	200	200	217
129	130	140	130	133
147	200	220	250	223
156	250	250	250	250
170	180	200	210	197
171	150	160	160	157
188	160	160	160	160
210	200	220	200	207
220	180	150	120	150
232	250	250	250	250
249	250	250	250	250
266	180	160	200	180
350	400	400	400	400
361	250	250	300	267
398	400	400	400	400
400	400	400	400	400
450	400	400	400	400
470	400	400	400	400

**Table S1.** ALT whole blood raw data

Roche Analyzer Value (U/L)	Paper Test Value Reader 1 (U/L)	Paper Test Value Reader 2 (U/L)	Paper Test Value Reader 3 (U/L)	Paper Test Value Average (U/L)
11	40	40	60	47
14	40	40	40	40
16	40	60	40	47
17	40	70	50	53
21	40	40	60	47
21	40	40	40	40
24	60	60	60	60
28	40	40	40	40
28	40	60	40	47
28	80	40	40	53
29	40	40	60	47
30	80	80	80	80
34	60	40	60	53
34	40	40	30	37
34	40	50	40	43
36	40	60	70	57
37	60	60	40	53
40	40	40	40	40
40	40	40	40	40
41	60	90	90	80
41	40	60	40	47
42	60	80	80	73
44	40	40	40	40
44	40	40	60	47
45	60	60	60	60
46	80	60	40	60
47	40	40	40	40
47	100	100	90	97
48	90	80	60	77
49	60	40	40	47
49	70	40	80	63
49	80	60	60	67
49	80	80	100	87
53	60	40	80	60
53	60	30	90	60
54	80	70	60	70
54	100	100	95	98
55	40	80	60	60
56	40	40	60	47
58	80	80	90	83
59	60	60	40	53
61	60	40	90	63
61	80	90	80	83
63	60	60	60	60
66	120	100	120	113
66	80	80	60	73

68	80	40	60	60
70	100	100	100	100
70	90	80	110	93
71	60	80	60	67
74	40	40	40	40
76	90	90	100	93
79	60	80	80	73
80	90	90	90	90
80	80	90	90	87
82	90	80	100	90
90	180	150	150	160
96	110	90	100	100
97	60	80	80	73
100	80	60	90	77
101	80	60	50	63
102	80	90	60	77
103	60	80	70	70
103	100	100	110	103
111	110	120	120	117
112	110	120	100	110
114	100	90	90	93
117	60	60	80	67
119	100	90	100	97
120	150	150	130	143
123	80	80	60	73
125	100	100	80	93
133	150	130	120	133
134	100	100	100	100
138	100	100	70	90
147	130	200	180	170
155	180	140	110	143
155	150	120	140	137
160	180	180	130	163
163	180	200	180	187
166	130	140	130	133
166	120	100	90	103
168	180	250	180	203
173	120	120	120	120
176	130	130	140	133
181	130	150	130	137
194	300	250	300	283
204	200	300	200	233
218	300	250	300	283
226	180	150	180	170
350	400	400	400	400
396	400	400	300	367
450	400	400	400	400
490	400	400	400	400





42	40	40	40	40	40	40	40	40	40	40	40	40	40
42	40	40	40	40	40	40	40	40	40	40	40	40	40
42	40	60	60	50	40	40	40	40	40	60	40	60	48
45	60	40	40	60	60	60	60	40	60				53
46	60	80	80										73
47	60	60	80	40	60	60	40	60	60	40	60	60	57
47	40	40	40										40
47	40	40	60										47
50	40	80	80	60	60	60	60	40	60	60	40	60	58
50	110	90	100										100
51	100	90	100										97
53	40	60	100	40	40	60	40	40	60	40	40	60	52
53	20	40	40										33
55	100	100	100										100
56	40	60	40	40	40	60	60	60	80	50	40	60	53
56	40	60	40	40	40	40	40	60	40	40	40	40	43
58	100	80	90										90
60	80	80	80										80
65	40	20	40	80	80	60	80	80	60	70	80	60	63
66	80	80	80	60	40	60	60	60	80	60	60	80	67
68	20	40	40	60	40	60	60	40	60	60	40	60	48
68	60	80	80										73
70	40	70	60										57
74	90	60	80	80	80	80	80	60	80	80	40	60	73
74	100	100	160										120
75	40	20	40	40	20	40	40	20	40	40	20	40	33
78	60	60	60	60	60	60	60	40	60	60	40	60	57
79	100	110	120	60	80	80	60	80	80	60	80	60	81
79	60	60	60	60	60	70	60	60	80				63
80	110	60	80	40	20	40	60	40	40	60	60	60	56
80	40	40	40	40	40	40	40	40	40				40
81	80	70	110	90	120	110	100	130	120	90	120	110	104
84	80	100	100	80	100	100	80	100	100	60	100	100	92
84	80	80	100										87
84	60	60	100										73
85	80	80	120	80	130	120	90	130	120	80	130	120	107
85	120	80	80	100	80	80	100	80	80				88
89	70	100	80	70	90	80	70	80	80				80
99	130	80	110	100	130	120	100	120	100	80	120	100	108
101	60	60	60	40	20	40	40	20	40	40	20	40	40
104	80	60	inv	70	80	100	70	80	100	70	80	100	81
104	40	40	40	40	40	40	40	40	40				40
105	60	80	100	60	100	100	80	100	100	80	100	80	87
105	120	130	160	80	100	100	100	100	100	100	100	100	108
106	20	40	60										40
107	40	40	60	40	40	40	40	40	60	50	40	60	46
107	100	90	130	100	100	130	100	80	130				106
108	60	80	100	80	100	120	40	40	120	60	100	120	85

108	40	40	30										37
110	90	90	130	80	100	100	60	80	100	60	80	100	89
115	40	50	80	80	120	120	100	130	120	100	130	120	99
117	120	120	160										133
118	180	140	180	120	180	160	150	180	180	100	160	150	157
122	110	100	110	120	100	120	120	100	120				111
122	100	100	110	120	100	120	100	100	100				105
124	200	180	200										193
124	120	120	100	120	120	100	120	120	120				115
128	120	120	100	120	110	100	100	100	80				105
129	110	100	110										107
147	120	120	120	60	80	80	120	150	120	120	120	120	111
156	110	130	160										133
170	200	180	180										187
171	100	100	130	100	120	120	80	120	110	inv	inv	inv	109
179	100	140	130	100	130	130	100	130	130				121
188	130.00	120.00	130.00										127
210	250	250	200										233
220	150	150	200	180	200	200	180	200	200	250	200	200	193
232	400	400	250										350
241	120	120	130	120	120	150	120	120	130				125
249	250	250	200	180	200	200	200	200	200	250	200	200	211
255	130	130	170	120	180	200	100	160	160	150	200	200	158
266	120	110	180	250	250	250	250	250	200	inv	inv	inv	207
316	200	200	180	180	190	150	200	190	180				185
316	250	200	190	250	200	200	250	180	190				212
318	200	200	140	250	250	160	200	200	140				193
361	250	250	300										267
398	250	250	250										250
400	400	400	400	250	200	250	300	250	250	300	250	250	292
419	200	250	250	250	250	250	250	250	250				244
423	300	250	200	250	200	200	300	300	250				250
425	400	400	400	400	400	400	400	400	400	inv	inv	inv	400
450	400	400	400	250	250	250	250	250	250	200	250	250	283
450	400	400	250	250	400	400	200	400	200	250	400	400	329
470	400	400	400										400

**Table S3.** ALT serum raw data. R1, R2, and R3 refer to Reader 1, Reader 2, and Reader 3, respectively. Paper Test A-D refers to 4 independent tests used to measure the same sample. Blank cells indicate that an insufficient volume of serum was available for all repeats. Inv = result was invalid due to sample hemolysis.

	Paper Test A (U/L )			Paper Test B (U/L)			Paper Test C (U/L)			Paper Test D (U/L)			
Roche Analyzer Value (U/L)	R1	R2	R3	R1	R2	R3	R1	R2	R3	R1	R2	R3	Average Paper Test Value (U/L)
11	40	70	60										57
14	30	40	40	40	40	60	40	40	40	40	40	40	41
16	70	80	60										70
17	40	40	40										40
21	40	40	40										40
21	40	40	40										40
23	60	80	60	60	40	40	60	40	40	inv	inv	inv	53
24	60	40	60	40	40	40	40	40	40	40	40	40	43
25	40	40	40	40	40	40	60	40	40				42
26	40	40	40	40	40	40	40	40	80				44
28	60	60	40	40	40	40	40	40	40	40	40	40	43
28	40	40	40	40	40	40	40	40	40	40	40	40	40
28	40	40	40	60	60	60	60	60	60	60	60	60	55
29	40	40	40	40	40	40	40	40	40	40	40	40	40
30	40	40	40										40
30	40	40	60	40	40	60	60	40	80				51
34	100	90	100										97
34	90	60	60										70
36	150	200	100										150
37	60	40	40	40	40	40	40	40	40	40	40	40	42
37	50	40	40										43
40	40	80	60	40	80	60	40	80	60	40	80	60	60
40	40	40	40										40
41	90	100	80										90
41	40	40	60										47
42	40	80	150										90
44	50	60	40	40	40	40	40	40	40	40	40	40	43
44	90	100	90	40	40	60	40	40	60	40	40	60	58
44	40	40	60										47
44	40	80	60	40	80	40	60	80	60				60
44	60	40	60	60	40	60	80	40	80				58
45	50	50	40	40	40	40	40	40	40	40	40	40	42
46	40	40	40	40	40	60	40	40	60	40	40	60	45
46	40	80	60	40	80	60	40	80	60				60
47	80	40	90	40	80	60	40	80	60	40	80	60	63
47	90	90	80										87
48	40	50	40										43
49	80	80	90	40	40	40	40	40	40	40	40	40	51
49	60	40	40	40	40	40	40	40	40	40	40	40	42
49	80	70	80	60	60	40	60	60	40	60	60	40	59



120	150	160	150										153
123	100	100	100										100
125	120	180	150	120	120	150	100	100	120	100	120	120	125
125	120	120	150	120	150	150	120	120	150				133
126	100	100	80	100	100	100	100	100	80				96
133	150	150	180										160
134	90	90	80	110	120	150	150	300	180	250	300	200	168
136	100	100	90	100	100	90	100	100	100				98
138	200	210	200										203
147	200	250	200	120	120	120	180	180	180	180	200	180	176
152	150	180	200	120	120	150	120	180	180				156
155	200	250	200	300	300	200	180	200	120	300	400	200	238
155	220	190	180										197
158	120	120	120	150	150	130	150	120	150				134
160	180	160	150										163
162	150	180	180	150	180	150	150	180	180				167
163	200	210	200										203
166	150	150	180	200	180	150	200	180	150	200	300	300	195
166	250	190	180										207
168	200	300	300	400	400	400	400	400	400	400	400	300	358
173	180	400	200	400	400	400	400	400	300	400	400	300	348
174	400	300	300	400	300	400	300	300	300				333
176	300	400	300	400	400	300	400	400	300	400	400	200	350
181	220	210	180										203
194	180	250	300	400	400	200	400	400	200	400	400	300	319
196	300	250	300	300	300	200	300	250	300				278
204	180	200	180	180	180	180	120	120	120	250	300	200	184
218	400	400	400	300	300	200	300	300	300	300	300	300	317
226	300	300	200										267
278	400	400	300	300	400	400	300	400	300				356
293	300	400	400	400	400	400	300	400	400				378
376	400	400	400	300	400	300	400	400	300				367
383	400	400	300	400	400	300	400	400	400				378
396	400	400	400										400
400	400	400	400	400	400	400	400	400	400	400	400	400	400
425	400	400	400	400	400	400	400	400	400	400	400	400	400
450	400	400	400	400	400	400	400	400	400	400	400	400	400
463	400	300	400	400	300	400	400	300	300				356
470	400	400	400										400
490	400	400	400										400

**Table S4.** AST serum raw data. R1, R2, and R3 refer to Reader 1, Reader 2, and Reader 3, respectively. Paper Test A–D refers to 4 independent tests used to measure the same sample.

Blank cells indicate that an insufficient volume of serum was available for all repeats. Inv = result was invalid due to sample hemolysis.

<b>Total Manufacturing Equipment &amp; Personnel</b>		<b>\$0.0049</b>
<b>Consumable</b>		
Whatman Chromatography Paper		\$0.0025
Wax for wax printer		\$0.0008
Laminate Coating		\$0.0005
Adhesive (Unitak 131)		\$0.0004
Filter Membrane		\$0.0250
Foil-lined Pouch (100 devices/pack)		\$0.0075
Dessicant (1 pack/100 devices)		\$0.0075
Reagents (Enzymes, Chemistry, etc)		\$0.0225
<b>Total Consumable</b>		<b>\$0.0667</b>
<b>Total Cost</b>		<b>\$0.0715</b>

**Table S5.** Cost Per Device Estimate of Paper-based Transaminase Test. Manufacturing costs are based on estimated infrastructure and personnel costs for India (costs for similar manufacturing in the US would be 2-3X higher). Consumable pricing based on cost of materials currently being incurred at the research level and adjusted for lower prices based on volume discount. Infrastructure costs include building, setting up manufacturing line, etc.